First-principles calculations of tunneling conductance

H. Ishida,[1] D. Wortmann,[2] and T. Ohwaki[2]
[1]*College of Humanities and Sciences, Nihon University, Sakura-josui, Tokyo 156-8550, Japan*
[2]*Research Institute for Computational Science, AIST, Tsukuba, Ibaraki 306-8568, Japan*
(Received 31 March 2004; published 24 August 2004)

Based on the embedding Green function method, we present a formula to calculate the current through a tunnel barrier. In contrast to the Landauer equation, our approach incorporates not only the contribution of propagating bulk states but also tunneling from localized states. As a first example, field emission from Cu surfaces and electronic transport in a Cu-vacuum-Cu system are presented.

DOI: 10.1103/PhysRevB.70.085409 PACS number(s): 73.40.−c, 71.15.Ap, 72.10.−d, 73.20.At

I. INTRODUCTION

Tunneling of electrons through a potential barrier is a subject in elementary quantum mechanics. Nevertheless, electron tunneling within one-electron theory is an essential concept relevant to a number of technological applications such as field-emitting devices,[1] tunnel devices using magnetic tunnel junctions,[2,3] those using semiconductor heterostructures,[4] and scanning tunneling microscopy.[5] With the advance in experimental techniques to control the structure of those devices on the atomic scale, there is an increasing demand in establishing a theoretical framework for evaluating the tunnel current microscopically in terms of the electronic structure of realistic materials.

In this paper we restrict ourselves to the one-electron approximation within the density-functional theory,[6,7] without considering many-body effects such as the Coulomb blockade.[8,9] Previous first-principles calculations of the tunnel current are classified into those based on the scattering theory[10–17] and those based on the perturbation theory initiated by Bardeen.[18–23] In the former, tunneling is described as a scattering process in which an incident electron wave is scattered by a barrier potential located between two semi-infinite bulk systems. The tunnel current is evaluated from the transmission amplitude of scattered electron waves using the Landauer-Büttiker formula.[24,25] In the latter, two systems on both sides of the potential barrier are treated as decoupled in the initial state, and the probability for electrons to tunnel through the potential barrier is calculated by perturbation theory using Fermi's golden rule. As an advantage of nonperturbative theory, the scattering approach can treat both tunneling and ballistic conduction regimes, while the applicability of the perturbation approach is limited to small tunneling rates. As a disadvantage, the Landauer-Büttiker formula fails to incorporate the contribution to the tunnel current from localized (surface) states on one side of the potential barier to an energy continuum on the other side of the barrier, whereas there is no distinction between localized and extended states in Bardeen's perturbation treatment.[18]

The purpose of the present paper is to develop a method for evaluating the tunnel current from both extended and localized states by applying a single formula. From a view point of the way of solving the Schrödinger equation, our method belongs to the scattering formalism in which a potential barrier and two semi-infinite bulk systems (electrodes) on both sides are treated as a whole. Also, we adopt the Landauer-Büttiker formula[24,25] for evaluating the tunnel current from states extended in the whole system. In addition we explicitly incorporate the contribution of localized states to the total current. When a localized surface state formed in a semi-infinite bulk system on one side of the potential barrier is coupled to an energy continuum at the other side, it becomes a resonance, and the tunnel current from this state to the energy continuum can be estimated from its lifetime. It will be shown that both contributions to the tunnel current can be expressed naturally in terms of the embedding potential invented by Inglesfield.[26,27] Furthermore, we will show that the two contributions can be seamlessly integrated into a single formula by carefully choosing the surface on which the current is calculated.

The plan of the paper is as follows. In Sec. II we begin with the definition of the embedding potential and formulate the tunneling conductance in the language of the embedding theory.[26,27] In Sec. III we apply the same formula for realistic materials. Results are presented of the first-principles calculation of field-emission currents from low-index Cu surfaces and the electronic transport in a Cu-vacuum-Cu system. Finally, a summary is given in Sec. IV. We use the Hartree atomic units throughout the paper unless otherwise stated.

II. THEORY

A. Embedding potential

We consider tunneling of electrons through a potential barrier Ω separating the left half space V_L and the right one V_R. The z axis is chosen such that the asymptotic regions of V_L and V_R correspond to $z=-\infty$ and $z=+\infty$, respectively (see Fig. 1). Within the one-electron approximation, electron

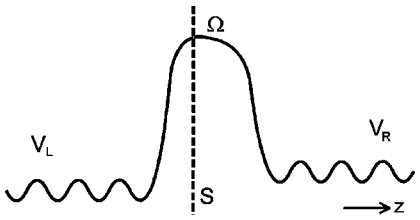

FIG. 1. Setup used for the calculation of tunnel currents. Potential barrier Ω separates two semi-infinite bulk systems, V_L and V_R. The tunnel current is evaluated on S, a boundary surface between V_L and V_R.

wave functions with energy ϵ satisfy the Schrödinger equation

$$\left[-\tfrac{1}{2}\Delta + v(\boldsymbol{r}) - \epsilon\right]\phi(\boldsymbol{r}) = 0. \tag{1}$$

Here $v(\boldsymbol{r})$ denotes the one-electron potential defined in the entire space. Another quantity that we will heavily use in this paper is the Green function

$$\left[-\tfrac{1}{2}\Delta + v(\boldsymbol{r}) - \epsilon\right]G(\boldsymbol{r},\boldsymbol{r}',\epsilon) = -\delta(\boldsymbol{r}-\boldsymbol{r}'). \tag{2}$$

Several Green functions corresponding to different boundary conditions can be defined. Hereafter, G is understood to express the retarded Green function defined in the whole space, satisfying the outgoing boundary conditions at $z=\pm\infty$. The imaginary part of such a Green function is related to the spectral function (density matrix) of the system by

$$\rho(\boldsymbol{r},\boldsymbol{r}',\epsilon) = -\frac{1}{\pi}\Im G(\boldsymbol{r},\boldsymbol{r}',\epsilon), \tag{3}$$

Green functions fulfilling other boundary conditions will be distinguished by putting a subscript to G.

In order to calculate the tunneling conductance, we define S, a two-dimensional (2D) surface separating V_L and V_R. S may be either a plane or a curved surface. For the time being, we do not specify the position of S. S can be either to the left, or to the right, or in the middle of the potential barrier Ω. We begin with the definition of the embedding potential introduced by Inglesfield.[26,27] Consider a Green function G_R at energy ϵ defined in V_R with a vanishing normal derivative on S and the outgoing boundary condition at $z=+\infty$. The surface inverse of G_R on S, which will be denoted by Σ_R, is called the embedding potential for the right half space V_R. Σ_R relates the value and normal derivative on S of any solution of Eq. (1), which is defined in V_R and satisfies the outgoing boundary condition at $z=+\infty$, by

$$\partial_n\phi(\boldsymbol{x}) = 2\int_S d\boldsymbol{x}'\Sigma_R(\boldsymbol{x},\boldsymbol{x}',\epsilon)\phi(\boldsymbol{x}'), \tag{4}$$

where the surface normal n points inward to V_R. In the same way we define Σ_L, the embedding potential for the left half space V_L.

By using a Green-function matching technique[28,29] or using the cusp condition of the Green function,[30] one can show easily that the Green function $G(\boldsymbol{x},\boldsymbol{x}',\epsilon)$ on S can be expressed using the embedding potentials by

$$G = G_L\frac{1}{G_L+G_R}G_R = \frac{1}{\Sigma_L+\Sigma_R}, \tag{5}$$

where we omit for simplicity the arguments of the Green functions and the product of Green functions implies matrix multiplication on S. From Eq. (5) one sees that the spectral function on S can be decomposed into the left spectral function ρ_L and the right one ρ_R, with each defined by

$$\rho_L = \frac{1}{\pi}G\Im\Sigma_L G^*, \quad \rho_R = \frac{1}{\pi}G\Im\Sigma_R G^*. \tag{6}$$

ρ_L and ρ_R express the contribution of propagating waves incident from $z=-\infty$ and $z=+\infty$ to the spectral function, respectively.[31,17] In addition, the spectral function may have δ-function-like peaks corresponding to surface (interface) states on the real energy axis. As is seen from Eq. (5), they correspond to zeros of the determinant $|\Sigma(\epsilon)|$ where $\Sigma\equiv\Sigma_L+\Sigma_R$. It is to be noted that the decomposition of ρ into the sum of ρ_L and ρ_R is not adequate for those poles, since both $\Im\Sigma_L$ and $\Im\Sigma_R$ vanish in the energy gap region where surface (interface) states appear.

B. Landauer-Büttiker formula

In the ballistic regime in which the electron mean free path is much larger than the thickness of Ω, the tunneling conductance can be expressed by the Landauer-Büttiker formula,[24,25]

$$\Gamma_{\mathrm{LB}}(\epsilon) = \frac{1}{2\pi}\sum_{i,j}|t_{ij}|^2, \tag{7}$$

where t_{ij} is the transmission coefficient between ϕ_{Li}, an incident channel with energy ϵ in V_L, and ϕ_{Rj}, a transmitted channel in V_R, both of which are normalized such that they carry unit current toward the right. In the past the same formula was derived by a number of authors using linear response theories[32,33] and nonequilibrium Green-function techniques.[34–37] Recently, Wortmann *et al.*[30,38] reformulated Eq. (7) using the embedding technique as

$$\Gamma_{\mathrm{LB}}(\epsilon) = \frac{2}{\pi}\mathrm{Tr}[G\Im\Sigma_L G^*\Im\Sigma_R], \tag{8}$$

where all the matrices are defined on S. Here we give a simplified derivation of the earlier equation. To this end, we notice that the left spectral function can be written on S as

$$\rho_L(\boldsymbol{x},\boldsymbol{x}',\epsilon) = \frac{1}{2\pi}\sum_i\sum_{\nu,\nu'}[t_{i\nu}\phi_{R\nu}(\boldsymbol{x})]^*[t_{i\nu'}\phi_{R\nu'}(\boldsymbol{x}')], \tag{9}$$

where the sum over i runs through incident channels ϕ_{Li} while those over ν and ν' run through not only propagating but also evanescent solutions of Eq. (1) toward $z=+\infty$. We define an expectation value of the normal component of the current operator on S by

$$\begin{aligned} J_{\nu\nu'} &= \frac{1}{2i}\int_S[\phi^*_{R\nu}\,\partial_n\phi_{R\nu'} - \partial_n\phi^*_{R\nu}\phi_{R\nu'}]d\boldsymbol{x} \\ &= 2\int_S \phi^*_{R\nu}(\boldsymbol{x})\Im\Sigma_R(\boldsymbol{x},\boldsymbol{x}')\phi_{R\nu'}(\boldsymbol{x}')d\boldsymbol{x}d\boldsymbol{x}', \end{aligned} \tag{10}$$

where we used Eq. (4) in the second line.[30] The value of $J_{\nu\nu'}$ is independent of the shape and position of S, and vanishes when either $\phi_{R\nu}$ or $\phi_{R\nu'}$ is an evanescent state. When both are propagating waves, we adopt the eigenchannel normalization $J_{jj'}=\delta_{jj'}$. Combining Eqs. (9) and (10) yields

$$2\mathrm{Tr}[\rho_L\Im\Sigma_R] = \frac{1}{2\pi}\sum_{i\nu\nu'}t^*_{i\nu}t_{i\nu'}J_{\nu\nu'} = \frac{1}{2\pi}\sum_{ij}|t_{ij}|^2. \tag{11}$$

Thus, we have

$$\Gamma_{\mathrm{LB}}(\epsilon) = 2\ \mathrm{Tr}[\rho_L\ \Im\Sigma_R] = 2\int_S \rho_L(\boldsymbol{x},\boldsymbol{x}',\epsilon)\Im\Sigma_R(\boldsymbol{x}',\boldsymbol{x},\epsilon)d\boldsymbol{x}d\boldsymbol{x}', \tag{12}$$

which is seen to coincide with Eq. (8) using Eq. (6). Needless to say, Γ_{LB} can be expressed also as $2\mathrm{Tr}[\rho_R\Im\Sigma_L]$ by exchanging R and L.

As an application, let us consider field emission (FE) of electrons from a metal electrode. In this case, $v(\boldsymbol{r})$ consists of a crystal potential representing a semi-infinite metal electrode (V_L), a surface potential barrier, and a linearly decreasing potential in the vacuum (V_R). We take S as a plane located slightly outside the outermost atomic layer and assume that the potential barrier to the right of S depends only on the z coordinate. Then, noting that the embedding potential for a one-dimensional (1D) potential barrier can be written as

$$\Im\Sigma_R(\boldsymbol{x}',\boldsymbol{x},\epsilon) = \int \frac{d\boldsymbol{k}}{(2\pi)^2}\mathrm{e}^{i\boldsymbol{k}(\boldsymbol{x}'-\boldsymbol{x})}\Im\Sigma_R(\epsilon_\perp), \tag{13}$$

with $\epsilon_\perp = \epsilon - |\boldsymbol{k}|^2/2$, one has

$$\Gamma_{\mathrm{LB}}(\epsilon) = 2\int \frac{d\boldsymbol{k}}{(2\pi)^2}\rho_L(\boldsymbol{k},\boldsymbol{k},\epsilon)\Im\Sigma_R(\epsilon_\perp), \tag{14}$$

where $\rho_L(\boldsymbol{k},\boldsymbol{k},\epsilon)$ in Eq. (14) denotes the diagonal component of the Fourier transform of the left spectral function on S. The earlier equation coincides with an extended version of the Fowler-Nordheim theory,[39–41]

$$\Gamma_{\mathrm{FN}}(\epsilon) = \int \frac{d\boldsymbol{k}}{(2\pi)^2}\rho_L(\boldsymbol{k},\boldsymbol{k},\epsilon)v_z(\epsilon,\boldsymbol{k})D_0(\epsilon_\perp)/2, \tag{15}$$

if $2\Im\Sigma_R$ is replaced by $v_z D_0/2$, where D_0 is the electron tunneling probability within the Wenzel-Kramers-Brillouin (WKB) approximation and v_z is the normal component of the electron velocity. It should be emphasized, however, that differently from such an approximate equation, Eq. (12) holds for any rapidly varying three-dimensional (3D) potential barrier Ω.

C. Tunnel current from surface states

A drawback of the Landauer-Büttiker formula is that it fails to account for the tunnel current from localized surface (interface) states. This is known to make a significant contribution to the total current in scanning tunneling microscopy (STM)[5] and field emission.[41,42] To be concrete, let us consider an interface between a semi-infinite crystal occupying V_L and the semi-infinite vacuum V_R. Without a tip (STM), or without an applied electric field (FE), discrete surface states may appear below the vacuum level ($\Im\Sigma_R = 0$) in the energy gaps of the band structure of the crystal ($\Im\Sigma_L = 0$). As stated before, their energies are determined by the condition $|\Sigma(\epsilon)| = 0 (\Sigma = \Sigma_L + \Sigma_R)$. Now, when a tip approaches the surface (STM), or when an external electric field is applied (FE), these surface states couple with the energy continuum in the right half space and become surface resonances with a finite lifetime τ. We assume that the resupply of electrons into them via electron-electron interactions proceeds much faster than the tunneling from those states into the energy continuum in the tip (STM) or in the vacuum (FE), which may be justified for metallic substrates. With this assumption, the contribution of a surface state to the tunneling conductance is given by[42]

$$\Gamma_s(\epsilon) = \frac{1}{\tau}\delta(\epsilon - \epsilon_s) = 2\gamma\ \delta(\epsilon - \epsilon_s), \tag{16}$$

where ϵ_s and γ denote the center and half width at half maximum of the resonance peak, respectively. To proceed, we need to express γ in the language of embedding theory.

First, we give an intuitive derivation, though it is not necessarily rigorous. Let us denote the wave function of a localized surface state in the limit of $\gamma = 0$ corresponding to energy ϵ_s^0 by ϕ_s. Its coupling to the energy continuum in the right half space can be expressed as a change in $\Sigma(\epsilon)$ on S. We write $\Sigma(\epsilon) = \Sigma^0(\epsilon) + \Delta\Sigma(\epsilon)$, where $\Sigma^0(\epsilon)$ is the sum of the two embedding potentials when $\gamma = 0$. Since the negative of the embedding potential is a "potential energy" acting on surface S, the energy shift of this surface state is given by first-order perturbation theory as

$$\Delta\epsilon_s = -\int_S \phi_s^*(\boldsymbol{x}')\Delta\Sigma(\boldsymbol{x}',\boldsymbol{x},\epsilon_s^0)\phi_s(\boldsymbol{x})d\boldsymbol{x}d\boldsymbol{x}'. \tag{17}$$

When $\Delta\Sigma$ is switched on, surface-state poles on the real energy axis shift to the lower half of the complex energy plane. Thus, γ is estimated from the imaginary energy of the pole, i.e.:

$$\gamma = \int_S \phi_s^*(\boldsymbol{x}')\Im\Sigma_R(\boldsymbol{x}',\boldsymbol{x},\epsilon_s^0)\phi_s(\boldsymbol{x})d\boldsymbol{x}d\boldsymbol{x}', \tag{18}$$

where we made use of the facts that $\Im\Sigma_L(\epsilon) = \Im\Sigma_R^0(\epsilon) = 0$ in the energy range of the resonance and that the embedding potential is permutable with respect to $\boldsymbol{x}$ and $\boldsymbol{x}'$.

A more rigorous derivation of γ is to determine the shift of a zero of the determinant. To the lowest order, we have

$$\begin{aligned}
&|\Sigma^0(\epsilon_s^0 + \Delta\epsilon_s) + \Delta\Sigma(\epsilon_s^0 + \Delta\epsilon_s)| \\
&\quad = \left|\Sigma^0(\epsilon_s^0) + \left[\frac{\partial\Sigma^0(\epsilon_s^0)}{\partial\epsilon}\Delta\epsilon_s + \Delta\Sigma(\epsilon_s^0)\right]\right| \\
&\quad = \mathrm{Tr}\left\{\Sigma_{\mathrm{adj}}^0(\epsilon_s^0)\left[\frac{\partial\Sigma^0(\epsilon_s^0)}{\partial\epsilon}\Delta\epsilon_s + \Delta\Sigma(\epsilon_s^0)\right]\right\} = 0,
\end{aligned} \tag{19}$$

where $\Sigma_{\mathrm{adj}}^0(\epsilon)$ is the adjoint matrix of $\Sigma^0(\epsilon)$ and we used $|\Sigma^0(\epsilon_s^0)| = 0$ in the third line. Since the Green function on S in the limit of $\gamma = 0$, $G^0(\epsilon) = (\Sigma^0)^{-1}(\epsilon) = \Sigma_{\mathrm{adj}}^0(\epsilon)/|\Sigma^0(\epsilon)|$, can be written as

$$G^0(\epsilon) = \frac{\phi_s(\boldsymbol{x})\phi_s^*(\boldsymbol{x}')}{\epsilon - \epsilon_s^0}, \tag{20}$$

in the neighborhood of ϵ_s^0, $\Sigma_{\mathrm{adj}}^0(\epsilon_s^0)$ in Eq. (19) is seen to be identical with $\phi_s(\boldsymbol{x})\phi_s^*(\boldsymbol{x}')$ except for a constant $\partial|\Sigma^0(\epsilon_s^0)|/\partial\epsilon$. Thus, Eq. (19) reads

$$\left[\int_S \phi_s^*(\boldsymbol{x}')\frac{\partial\Sigma^0(\boldsymbol{x}',\boldsymbol{x},\epsilon_s^0)}{\partial\epsilon}\phi_s(\boldsymbol{x})d\boldsymbol{x}d\boldsymbol{x}'\right]\Delta\epsilon_s = -\int_S \phi_s^*(\boldsymbol{x}')\Delta\Sigma(\boldsymbol{x}',\boldsymbol{x},\epsilon_s^0)\phi_s(\boldsymbol{x})d\boldsymbol{x}d\boldsymbol{x}'. \quad (21)$$

Here we utilize a property of the embedding potential[26]

$$\int_S \phi_s^*(\boldsymbol{x}')\frac{\partial\Sigma_L^0(\epsilon_s^0)}{\partial\epsilon}\phi_s(\boldsymbol{x})d\boldsymbol{x}d\boldsymbol{x}' = \int_{V_L}|\phi_s(\boldsymbol{r})|^2d\boldsymbol{r}, \quad (22)$$

$$\int_S \phi_s^*(\boldsymbol{x}')\frac{\partial\Sigma_R^0(\epsilon_s^0)}{\partial\epsilon}\phi_s(\boldsymbol{x})d\boldsymbol{x}d\boldsymbol{x}' = \int_{V_R}|\phi_s(\boldsymbol{r})|^2d\boldsymbol{r}. \quad (23)$$

Adding the earlier two equations for each side and noting the normalization condition $\int|\phi_s(\boldsymbol{r})|^2d\boldsymbol{r}=1$, one finds that the coefficient of $\Delta\epsilon_s$ on the left-hand side of Eq. (21) equals unity. Thus, Eq. (21) coincides with Eq. (17).

By substituting Eq. (18) in Eq. (16), we obtain

$$\Gamma_s(\epsilon) = 2\int_S [\phi_s(\boldsymbol{x})\phi_s^*(\boldsymbol{x}')\delta(\epsilon-\epsilon_s)]\Im\Sigma_R(\boldsymbol{x}',\boldsymbol{x},\epsilon)d\boldsymbol{x}d\boldsymbol{x}'. \quad (24)$$

As it should be, $\Gamma_s(\epsilon)$ evaluated by the earlier equation does not depend on the position of S. Now, we adopt an approximate expression of the spectral function in the energy range of a surface resonance

$$\rho(\boldsymbol{x},\boldsymbol{x}',\epsilon) = \phi_s(\boldsymbol{x})\phi_s^*(\boldsymbol{x}')\delta(\epsilon-\epsilon_s). \quad (25)$$

Strictly speaking, Eq. (25) is exact only in the limit of $\gamma=0$. However, its use for a finite γ may be justified for the present purpose, since the spectral function possesses a sharp peak centered at ϵ_s and its integrated weight in the energy range of the resonant peak deviates from $\phi_s(\boldsymbol{x})\phi_s^*(\boldsymbol{x}')$ only by an amount of the order of $\Delta\Sigma(\epsilon_s)$, as far as $\phi_s(\boldsymbol{x})$ has a significant amplitude on S.

When a surface state couples with the energy continuum in V_R, the resultant surface resonance is described as a part of the right spectral function ρ_R, while ρ_L remains to be zero in the energy gap of the crystal. Thus, from Eqs. (24) and (25) with ρ replaced by ρ_R, one has

$$\Gamma_s(\epsilon) = 2\int_S \rho_R(\boldsymbol{x},\boldsymbol{x}',\epsilon)\Im\Sigma_R(\boldsymbol{x}',\boldsymbol{x},\epsilon)d\boldsymbol{x}d\boldsymbol{x}'. \quad (26)$$

This equation is valid only for narrow energy windows corresponding to surface resonances. Except for these energies, $\Gamma_s(\epsilon)$ should vanish, while the right-hand side of Eq. (26) does not necessarily. However, one can make use of the fact that electron wave functions incident from $z=+\infty$ decay inside the potential barrier Ω except for resonance energies. So far, we have not specified the position of the boundary surface S between V_L and V_R. Now, we choose to position S on the left side of the potential barrier Ω. In this case, one may expect that $\rho_R\simeq 0$ on S if the amplitude of electron wave functions incident from $z=+\infty$ becomes sufficiently small before reaching S. Roughly speaking, the condition for this may be $\exp(-2\kappa L)\ll 1$, where κ is the decay constant in Ω of a wave function incoming from $z=+\infty$ and L denotes thickness of Ω. With this assumption, Eq. (26) may be a very good approximation of $\Gamma_s(\epsilon)$ in Eq. (24) for all the energies.

D. Formula for both bulk and surface currents

In the preceding subsections we discussed the tunneling currents from bulk and surface states. Now, as a tunneling-conductance formula that can account for both the contributions, we propose

$$\Gamma(\epsilon) = 2\ \mathrm{Tr}[\rho\ \Im\Sigma_R] = 2\int_S \rho(\boldsymbol{x},\boldsymbol{x}',\epsilon)\Im\Sigma_R(\boldsymbol{x}',\boldsymbol{x},\epsilon)d\boldsymbol{x}d\boldsymbol{x}'. \quad (27)$$

Using the definitions for $\Gamma_{\mathrm{LB}}(\epsilon)$ and $\Gamma_s(\epsilon)$ as given in Eqs. (12) and (26), respectively, Eq. (27) is rewritten as

$$\Gamma(\epsilon) = \Gamma_{\mathrm{LB}}(\epsilon) + \Gamma_s(\epsilon). \quad (28)$$

The assumption that $\rho=\rho_R+\rho_L$ used here is valid as we consider a finite coupling of the surface states to the energy continuum at the right side of the barrier. As $\Gamma_{\mathrm{LB}}(\epsilon)=0$ for the energies of the surface resonances, Eqs. (27) and (26) obviously give the same contribution of these states to the conductance. At energies in which a continuum of states is available at both sides, i.e., whenever $\Gamma_{\mathrm{LB}}(\epsilon)\neq 0$, the proposed formula contains an extra contribution Eq. (26). As described in the preceding subsection, this additional contribution can be tuned to practically vanish by positioning S at the left side of the barrier Ω, where the charge density due to the states incident from $z=+\infty$ becomes negligibly small.

To demonstrate this, we consider simplified 1D potential barriers for which the embedding potentials, Σ_R and Σ_L, can be analytically calculated. As the first example we take a rectangular potential barrier

$$v(z) = \begin{cases} 0 & (z\leqslant 0, z\geqslant D) \\ \epsilon_v & (0\leqslant z\leqslant D). \end{cases} \quad (29)$$

In Fig. 2(a) we plot the ratio of the proposed formula Eq. (27) to the Landauer-Büttiker formula Eq. (12) at three energies as a function of the z coordinate of S, where ϵ_v and D are chosen, as an example, as 0.5 and 5 a.u., respectively. As $\Gamma_{\mathrm{LB}}(\epsilon)$ does not depend on the position of S, the variation of these lines originates from the z dependence of Eq. (27). For a 1D model, the ratio is given by $\Gamma/\Gamma_{\mathrm{LB}}=1+\rho_R(z,z,\epsilon)/\rho_L(z,z,\epsilon)$ with z being the position of S. Since $\rho_R=\rho_L$ at $z=D/2$ for any symmetric potential barrier, all the lines pass through the point (2.5, 2). Main contributions to $\rho_R(z,z,\epsilon)$ and $\rho_L(z,z,\epsilon)$ behave in the barrier region as $\exp(+2\kappa z)$ and $\exp(-2\kappa z)$ with $\kappa=\sqrt{2(\epsilon_v-\epsilon)}$, respectively. As a result, $\Gamma/\Gamma_{\mathrm{LB}}$ diverges as $\exp(+4\kappa z)$ in the barrier region. As expected, near the left end of the barrier ($z\sim 0$), the ratio $\Gamma/\Gamma_{\mathrm{LB}}$ may be regarded practically as unity. Hence, one may use Eq. (27) to calculate the tunnel current from extended bulk states.

As the second model, we consider field emission from a 1D step potential

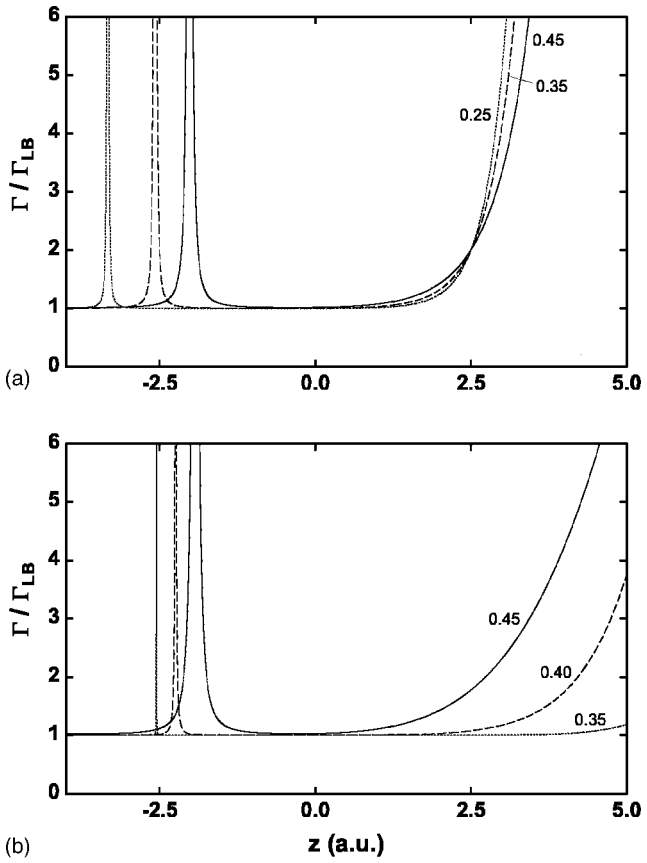

FIG. 2. $\Gamma(\epsilon)/\Gamma_{\mathrm{LB}}(\epsilon)$ as a function of the z coordinate of S. (a) Rectangular potential with $\epsilon_v=0.5$ a.u. and $D=5$ a.u. (b) Field emission from a 1D step potential with $\epsilon_v=0.5$ a.u. and $F=0.01$ a.u. Small numbers near each line indicate electron energy ϵ.

$$v(z)=\begin{cases}0 & (z\leqslant 0)\\ \epsilon_v - Fz & (z\geqslant D).\end{cases} \tag{30}$$

Figure 2(b) shows the calculated $\Gamma/\Gamma_{\mathrm{LB}}$ as a function of the z coordinate of S, where ϵ_v and F are taken, as an example, as 0.5 and 0.01 a.u., respectively. Since the width of the potential barrier increases with decreasing ϵ, Γ remains to be identical with Γ_{LB} further into the vacuum with decreasing ϵ. Again, Eq. (27) agrees with Γ_{LB} nearly perfectly if S is located near the left edge of the potential barrier ($z\sim 0$).

Very interestingly, $\Gamma/\Gamma_{\mathrm{LB}}$ in Figs. 2(a) and 2(b) also shows sharp peaks on the left side of the potential barrier. This can be understood as follows: To the left of the barrier, $\rho_L(z,z,\epsilon)$ can be written as $[(1-R)^2+4R\sin^2(kz+\eta)]/k$ where R and η denote the reflection amplitude and phase shift of a plane wave incoming from $z=-\infty$ and carrying unit current, $\exp(ikz)/\sqrt{k}$ with $k=\sqrt{2\epsilon}$, whereas $\rho_R(z,z,\epsilon)=(1-R^2)/k$ is constant. Thus, the ratio $\rho_R(z,z,\epsilon)/\rho_L(z,z,\epsilon)$ has peaks with a height $(1+R)(1-R)$ and a half width at the half maximum, $\Delta z=(1-R)/(2k\sqrt{R})$ with a period of π/k. As $R\rightarrow 1$, the peaks behave like a δ function. We emphasize, however, that this singular behavior is an artifact of a constant potential in V_L where both incoming and reflected waves are single plane waves. For realistic 3D systems, the reflected wave corresponding to a Bloch wave incident from $z=-\infty$ is a superposition of many Bloch and evanescent waves. Furthermore, a single Bloch wave consists of many plane waves. Thus, it does not happen that the amplitudes of the incident and reflected waves cancel each other completely on all the points on S.

Equation (27) conforms with an intuitive picture of the tunneling current as it is written as a product of two quantities, i.e., $\rho(\boldsymbol{x},\boldsymbol{x}',\epsilon)$, a measure of the number density of electrons on the left side of the potential barrier, and $\Im\Sigma_R$, a quantity related to the probability for an electron on S to tunnel from the left to the right side of the barrier. In such a picture, it is plausible that there is no distinction between the current expression due to bulk states and that due to surface states. Using a 1D potential model, Soven, Plummer, and Kar[42] showed that the FE current from surface states can be expressed by the same equation as that from bulk states. In their treatment, the width of a surface resonance, γ, was estimated from the phase shift of a plane wave incident from $z=+\infty$. The present result may be regarded as a generalization to 3D arbitrary potential barriers of their result.

Given the tunneling conductance $\Gamma(\epsilon)$, the total tunnel current from V_L to V_R can be calculated as

$$J=2\int_{\mu_R}^{\mu_L}\Gamma(\epsilon)d\epsilon, \tag{31}$$

where μ_L and $\mu_R(\mu_L>\mu_R)$ are the chemical potentials in two semi-infinite systems, V_L and V_R, respectively, and the prefactor 2 accounts for electron spin.

To conclude this section, we summarize advantages of the present formula $\Gamma(\epsilon)$ in Eq. (27): (i) Differently from Γ_{LB}, Γ contains both bulk and surface contributions to the tunnel current. Regarding the bulk component, Γ becomes identical with Γ_{LB} if $\rho_R\simeq 0$ on S. (ii) Differently from Bardeens' transfer Hamiltonian approach, Γ is nonperturbative as far as the tunneling current from bulk states is concerned. (iii) Γ relies on no approximation of the tunneling probability such as the WKB approximation.

III. RESULTS

As a first application of Eq. (27) to a realistic system, we consider field emission from Cu(001) and Cu(111) surfaces. Recently, Ohwaki *et al.*[43] reported a first-principles calculation of field emission from those surfaces. In their work, the tunnel current from extended bulk states and that from surface states were computed separately using Eqs. (8) and (16), while we will evaluate them at once using Eq. (27).

We determine the electronic structure of a semi-infinite crystal surface exposed to a strong electric field within the local density approximation[7] by employing a surface-embedded Green-function method combined with the full-potential linearlized-augmented-plane-wave technique.[44–46] In this method, one considers explicitly the surface region with a finite thickness, $b_1\leqslant z\leqslant b_2$, and the effects of the semi-infinite substrate and the semi-infinite vacuum are incorporated via complex embedding potentials acting on two embedding surfaces, $z=b_1$ and $z=b_2$. Two outermost Cu layers are included in the embedded region and the embedding

plane on the vacuum side is placed at a position where the charge density becomes negligibly small. The embedding potential of the substrate is generated from the complex band structure[16] of Cu, while that for the vacuum in the presence of an electric field is expressed in terms of the Airy functions.[41,43]

Once the self-consistent charge density and potentials are determined by a standard iteration procedure, we evaluate the tunnel current using Eq. (27). We choose S, the surface separating V_L and V_R, as a plane $z=b_s$ located slightly on the vacuum side of the muffintin (MT) spheres of the top Cu layer. The embedding potential Σ_R on S is computed by performing an additional embedded Green-function calculation in a smaller region, $b_s \leqslant z \leqslant b_2$. In doing so, one imposes the same embedding potential expressed in terms of the Airy functions on $z=b_2$, while the von Neumann boundary condition with a vanishing normal derivative is imposed on $z=b_s$. By definition, Σ_R is obtained as the surface inverse of this Green function on S.[26] Since the volume $b_s \leqslant z \leqslant b_2$ contains no MT spheres, one can use a plane-wave basis set for this additional embedding calculation. Due to the translational symmetry in the plane, the tunneling conductance in the present case can be written as

$$\Gamma(\epsilon) = \frac{A}{(2\pi)^2} \int_{\mathrm{SBZ}} \Gamma(\epsilon, \boldsymbol{k}) d\boldsymbol{k}, \tag{32}$$

where $\boldsymbol{k}$ denotes a 2D wave vector in the surface Brillouin zone (SBZ) and A is the surface area. The equation corresponding to Eq. (27) is

$$\Gamma(\epsilon, \boldsymbol{k}) = 2\ \mathrm{Tr}[\rho(\epsilon, \boldsymbol{k}) \Im \Sigma_R(\epsilon, \boldsymbol{k})], \tag{33}$$

where $\rho(\epsilon, \boldsymbol{k})$ and $\Sigma_R(\epsilon, \boldsymbol{k})$ are the $\boldsymbol{k}$-resolved spectral function and embedding potential defined on S, respectively. Both matrices are expanded on S with a basis set $\{\boldsymbol{k}+\boldsymbol{g}\}$, where $\boldsymbol{g}$ is a 2D reciprocal lattice vector according to the translational symmetry in the plane. Thus, calculating the trace in Eq. (33) is reduced to summation over two sets of 2D reciprocal lattice vectors. The total field-emission current is obtained by integrating $\Gamma(\epsilon)$ up to the Fermi energy of the substrate, ϵ_F.

The inset of Fig. 3 shows the calculated planar average of the self-consistent potential $v(\boldsymbol{r})$ for Cu(001). The field strength F is given by $F=4\pi\sigma$, where σ, surface charge per unit area, is taken as 10^{-3} a.u. This corresponds to $F=0.65$ V/Å. For the case of Cu(001), there are no occupied surface state close to the Fermi energy, and the field-emission current originates from bulk states in the Cu 4s band. The current-density distribution as a function of 2D wave vector $\boldsymbol{k}$ exhibits a single sharp peak centered at $\overline{\Gamma}(\boldsymbol{k}=0)$ as in the case of the free-electron model. The solid line in Fig. 3 shows the energy distribution of the field-emission current $\Gamma(\epsilon, \boldsymbol{k})$ at $\boldsymbol{k}=0$, which was computed using Eq. (33) on the plane $z=b_s$ indicated by a vertical line in the inset. For comparison we also evaluated the Landauer-Büttiker formula, $\Gamma_{\mathrm{LB}}(\epsilon, \boldsymbol{k})$, which is obtained by replacing $\rho(\epsilon, \boldsymbol{k})$ in Eq. (33) by the $\boldsymbol{k}$-resolved left spectral function $\rho_L(\epsilon, \boldsymbol{k})$. On the vertical scale of Fig. 3, $\Gamma_{\mathrm{LB}}(\epsilon, \boldsymbol{k})$ and $\Gamma(\epsilon, \boldsymbol{k})$ agree perfectly

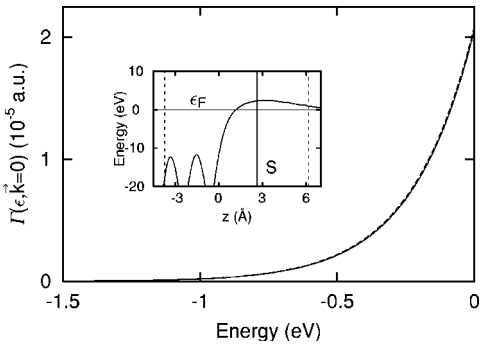

FIG. 3. $\boldsymbol{k}$-resolved tunneling conductance $\Gamma(\epsilon, \boldsymbol{k})$ at $\boldsymbol{k}=0$ for Cu(001) as a function of energy relative to the Fermi level ϵ_F (solid line). The dashed line is calculated with a broadening parameter $\delta = 5\times10^{-4}$ a.u. in the spectral function. The field strength $F=4\pi\sigma$, where σ is chosen as 10^{-3} a.u. The inset shows the planar average of the potential energy. The vertical solid line in the inset indicates the position of S.

and are not distinguishable from each other. This implies that our assumption that $\rho_L \gg \rho_R$ actually holds on the plane $z=b_s$.

Next we consider the Cu(111) surface. As was shown by Ohwaki *et al.*,[43] the field-emission current from Cu(111) is dominated by that from a partially occupied surface band that appears in the energy gap at the L point of the Cu band structure. The surface band has a minimum at $\boldsymbol{k}=0$ and exhibits nearly quadratic dispersion with $\boldsymbol{k}$. In the presence of an electric field, it becomes a surface resonance with a finite lifetime. At the same time its position shifts gradually downward with increasing field strength. Since there are no bulk states near ϵ_F at small $\boldsymbol{k}$, the bulk current from Cu(111) is much smaller than that for Cu(001).

To calculate the tunnel current from this surface band using Eq. (16), Ohwaki *et al.*[43] estimated the half width of the resonance at the half maximum, γ, by plotting the surface-layer density of states on very dense energy mesh points. This was an extremely time-consuming work, since the width of the resonance γ was only of the order of 10^{-6}–10^{-4} eV. In the present work we only have to integrate Eq. (33) up to the Fermi energy to obtain the tunnel current from both bulk and surface states. Though this is easier than evaluating the resonance width by hand, one still needs a dense energy mesh to be able to integrate the narrow surface resonance. To avoid this inconvenience, we propose to introduce an artificial broadening to the spectral function in Eq. (33) by replacing $\rho(\epsilon, \boldsymbol{k})$ by

$$\tilde{\rho}(\boldsymbol{x}, \boldsymbol{x}', \epsilon, \boldsymbol{k}) = -\frac{1}{\pi} \Im G(\boldsymbol{x}, \boldsymbol{x}', \epsilon + i\delta, \boldsymbol{k}). \tag{34}$$

The use of $\tilde{\rho}(\epsilon, \boldsymbol{k})$ may be justified as far as $\Im\Sigma_R(\epsilon, \boldsymbol{k})$ in Eq. (33) varies very little on the energy scale of δ.

In Fig. 4 we show the calculated tunneling conductance $\Gamma(\epsilon, \boldsymbol{k})$ at $\overline{\Gamma}(\boldsymbol{k}=0)$ for Cu(111) as a function of energy ϵ for three broadening parameters, $\delta=10^{-4}$, 5×10^{-4}, and 10^{-3} a.u. The field strength corresponds to $\sigma=10^{-3}$ (a.u.) The main peak in the figure corresponds to the surface resonance in the

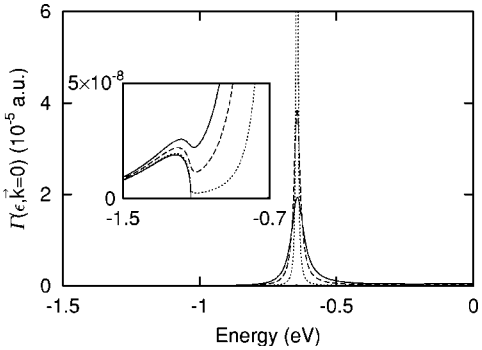

FIG. 4. $\boldsymbol{k}$-resolved tunneling conductance $\Gamma(\epsilon,\boldsymbol{k})$ at $\boldsymbol{k}=0$ for Cu(111) as a function of energy relative to the Fermi level ϵ_F. The solid, dashed, and dotted lines correspond to $\delta=10^{-3}$, 5×10^{-4}, and 10^{-4} a.u., respectively. The second solid line in the inset, which vanishes in the energy gap, is the Landauer-Büttiker formula $\Gamma_{\mathrm{LB}}(\epsilon,\boldsymbol{k})$.

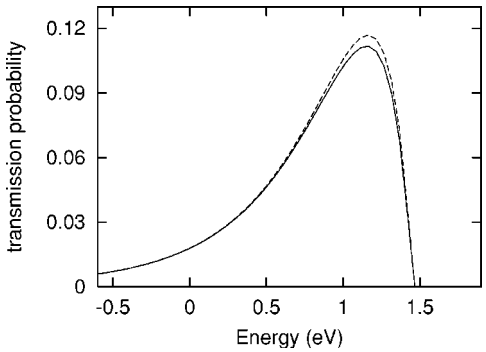

FIG. 5. Transmission probabilities according to Γ_{LB} (solid) and Γ (dashed) for a Cu(001)/vacuum/Cu(001) tunnel junction at $\boldsymbol{k}=0$ as a function of the electron energy $\epsilon(\epsilon_F=0)$.

energy gap of the Cu band structure. In order to show the contribution of bulk states to the tunnel current, we show the same function $\Gamma(\epsilon,\boldsymbol{k})$ with a magnified scale in the inset of Fig. 4. Though negligible as compared with the surface-resonance peak, one sees that bulk states contribute to the tunneling conductance up to the lower edge of the energy gap at $\overline{\Gamma}$. In the inset we also show the Landauer-Büttiker formula $\Gamma_{\mathrm{LB}}(\epsilon,\boldsymbol{k})$, which is seen to vanish identically in the energy gap. By integrating the surface-resonance peak, as the tunnel current at $\boldsymbol{k}=0$ we obtain 2.50×10^{-7}, 2.55×10^{-7}, and 2.65×10^{-7} a.u., for $\delta=10^{-4}$, 5×10^{-4}, and 10^{-3} a.u., respectively. These values are in good agreement with $2\gamma=2.48\times10^{-7}$ a.u., which was estimated from the width of the surface resonance without introducing an artificial broadening, although discrepancy increases slightly with increasing δ. The resonant peak in Fig. 4 can be integrated with a much coarser energy grid than γ. Thus, calculating the tunnel current from surface states becomes much easier by introducing $\delta>0$. The value of δ should be determined by balancing the numerical accuracy and computational amount.

Regarding the tunnel current from bulk states, one does not need to introduce such a broadening of the spectral function. However, since we would like to evaluate the tunnel currents from bulk and surface states at the same time using Formula Eq. (27), it may be worth examining the effect of δ on the bulk current. To see this, we show in Fig. 3 $\Gamma(\epsilon,\boldsymbol{k}=0)$ for Cu(001) calculated with a broadening parameter $\delta=5\times10^{-4}$ a.u. by a dashed line. By integrating this curve up to the Fermi level, one obtains the tunnel current which is overestimated only by 2% as compared with that calculated without a broadening (solid line).

As a further example we consider tunneling of electrons from a planar Cu(001) electrode through a vacuum layer with thickness 13.6 a.u. into another Cu(001) electrode. In this calculation we have chosen no additional surface S within the vacuum barrier but used the left embedding plane $z=b_1$ within the Cu electrode to evaluate Eq. (28) to avoid extra computational efforts and to demonstrate the validity of the discussion in Sec. II D for a 3D example. Figure 5 shows the tunneling probability of electrons with normal incidence ($\boldsymbol{k}=0$) calculated with the Landauer-Büttiker formalism as well as that obtained according to Eq. (28) with an additional factor 2π. In the energy range shown, the electronic structure of Cu has only single band of *sp* electrons and the tunneling probability increases exponentially until dropping to zero at the band edge at 1.46 eV. The transmission obtained from the two formulas agrees perfectly except for a small discrepancy at the high transmission values, which is expected as the additional contribution of $2\mathrm{Tr}[\rho_R\Im\Sigma_R]$ can no longer be neglected for a high transmissive junction. However, one should note that this deviation only occurs for very high tunneling rates.

IV. SUMMARY

In this paper we presented an efficient method to evaluate the tunnel current flowing between semi-infinite bulk systems separated by a potential barrier. Based on the embedding approach of Inglesfield, we derived not only the conductance due to tunneling of electrons from an energy continuum on one side to that on the other side of the potential barrier but also the conductance due to tunneling of electrons from localized states on one side to an energy continuum on the other side of the barrier. The former was obtained by reformulating the Landauer-Büttiker formula, while the latter was derived by expressing the lifetime of resonant states in terms of the embedding potential. Although they are based on different physics and assumptions, we have shown that both contributions can be seamlessly integrated into a single formula by carefully choosing the surface on which the tunnel current is evaluated. As a first application we calculated the field-emission current from Cu surfaces and the electronic transport in a Cu-vacuum-Cu system.

ACKNOWLEDGMENTS

This work was supported by the NAREGI Nanoscience Project, Ministry of Education, Culture, Sports, Science and Technology, Japan. D.W. thanks the Japan Science and Technology Agency for support.

[1] S. Fan, M. G. Chapline, N. R. Franklin, T. W. Tombler, A. M. Cassel, and H. Dai, Science **283**, 512 (1999).
[2] S. Yuasa, T. Nagahama, and Y. Suzuki, Science **297**, 234 (2002).
[3] R. Waser, *Nanoelectronics and Information Technology: Advanced Electronics Materials and Novel Devices* (Wiley, Weinheim, 2003).
[4] A. G. Petukhov, A. N. Chantis, and D. O. Demchenko, Phys. Rev. Lett. **89**, 107205 (2002).
[5] *Scanning Tunneling Microscopy III*, edited by R. Wiesendanger and H. J. Güntherodt (Springer, Berlin, 1996).
[6] P. Hohenberg and W. Kohn, Phys. Rev. **136**, B864 (1964).
[7] W. Kohn and L. J. Sham, Phys. Rev. **140**, A1133 (1965).
[8] R. Wilkins, E. Ben-Jacob, and R. C. Jaklevic, Phys. Rev. Lett. **63**, 801 (1989).
[9] W. Yi, L. Lu, H. Hu, Z. W. Pan, and S. S. Xie, Phys. Rev. Lett. **91**, 076801 (2003).
[10] N. D. Lang, Phys. Rev. Lett. **58**, 45 (1987).
[11] N. D. Lang, Phys. Rev. B **52**, 5335 (1995).
[12] K. Hirose and M. Tsukada, Phys. Rev. Lett. **73**, 150 (1994).
[13] K. Hirose and M. Tsukada, Phys. Rev. B **51**, 5278 (1995).
[14] C. Adessi and M. Devel, Phys. Rev. B **62**, R13 314 (2000).
[15] P. Mavropoulos, O. Wunnicke, and P. H. Dederichs, Phys. Rev. B **66**, 024416 (2002).
[16] D. Wortmann, H. Ishida, and S. Blügel, Phys. Rev. B **65**, 165103 (2002).
[17] M. Brandbyge, J. L. Mozos, P. Ordejón, J. Taylor, and K. Stokbro, Phys. Rev. B **65**, 165401 (2002).
[18] J. Bardeen, Phys. Rev. Lett. **6**, 57 (1961).
[19] J. A. Appelbaum and W. F. Brinkman, Phys. Rev. **186**, 464 (1969).
[20] J. Tersoff and D. R. Hamann, Phys. Rev. B **31**, 805 (1985).
[21] N. Isshiki, K. Kobayashi, and M. Tsukada, Surf. Sci. **238**, L439 (1990).
[22] C. J. Chen, Phys. Rev. B **42**, 8841 (1990).
[23] D. Wortmann, S. Heinze, P. Kurz, G. Bihlmayer, and S. Blügel, Phys. Rev. Lett. **86**, 4132 (2001).
[24] R. Landauer, Philos. Mag. **21**, 863 (1970).
[25] M. Büttiker, Phys. Rev. Lett. **57**, 1761 (1986).
[26] J. E. Inglesfield, J. Phys. C **14**, 3795 (1981).
[27] J. E. Inglesfield, Comput. Phys. Commun. **137**, 89 (2001).
[28] F. Garcia-Moliner and J. Rubio, J. Phys. C **2**, 1789 (1969).
[29] J. E. Inglesfield, Surf. Sci. **76**, 355 (1978).
[30] D. Wortmann, H. Ishida, and S. Blügel, Phys. Rev. B **66**, 075113 (2002).
[31] S. Datta, Superlattices Microstruct. **28**, 253 (2000).
[32] D. S. Fisher and P. A. Lee, Phys. Rev. B **23**, 6851 (1981).
[33] H. U. Baranger and A. D. Stone, Phys. Rev. B **40**, 8169 (1989).
[34] T. E. Feuchtwang, Phys. Rev. B **10**, 4121 (1974).
[35] C. Noguera, Phys. Rev. B **42**, 1629 (1988).
[36] Y. Meir and N. S. Wingreen, Phys. Rev. Lett. **68**, 2512 (1992).
[37] M. Brandbyge, N. Kobayashi, and M. Tsukada, Phys. Rev. B **60**, 17 064 (1999).
[38] O. R. Davies and J. E. Inglesfield, Prog. Surf. Sci. **74**, 161 (2003).
[39] A. Modinos, Solid-State Electron. **45**, 809 (2001).
[40] A. Modinos, J. Phys. C **9**, 3867 (1976).
[41] J. W. Gadzuk and E. W. Plummer, Rev. Mod. Phys. **45**, 487 (1973).
[42] P. Soven, E. W. Plummer, and N. Kar, CRC Crit. Rev. Solid State Sci. **6**, 111 (1976).
[43] T. Ohwaki, H. Ishida, and A. Liebsch, Phys. Rev. B **68**, 155422 (2003).
[44] H. Ishida, Phys. Rev. B **63**, 165409 (2001).
[45] J. E. Inglesfield and G. Benesh, Phys. Rev. B **37**, 6682 (1988).
[46] S. Crampin, J. B. A. N. van Hoof, M. Nekovee, and J. E. Inglesfield, J. Phys.: Condens. Matter **4**, 1475 (1992).